Contents lists available at ScienceDirect

Review of Palaeobotany and Palynology

Taxonomic and environmental significance of Poaceae and Cyperaceae phytoliths from the Northern Territory, Australia

Kelsey C. Boyd [a,b,*], Carlos E. Cordova [c], Haidee R. Cadd [a,b], Cassandra Rowe [d], Tim J. Cohen [a,b]

[a] School of Earth, Atmospheric, and Life Sciences, University of Wollongong, Wollongong 2522, New South Wales, Australia
[b] ARC Centre of Excellence for Australian Biodiversity and Heritage (CABAH), University of Wollongong, Wollongong 2522, New South Wales, Australia
[c] Department of Geography, Oklahoma State University, Stillwater, OK 74078, USA
[d] College of Science and Engineering, ARC Centre of Excellence of Australian Biodiversity and Heritage and Centre for Tropical Environmental and Sustainability Science, James Cook University, Cairns 4870, Queensland, Australia

ABSTRACT

Phytoliths are a valuable tool for reconstructing past grassy ecosystems. However, they are not commonly utilised as a palaeoecological proxy in Australia due to a lack of modern reference material from plants, particularly grasses. This study analyses phytolith reference material from 49 grass and 4 sedge species from the Northern Territory, Australia. This is used to develop a detailed classification scheme and multivariate morphospace analysis to examine taxonomic and ecological patterns of grass silica short cell phytolith (GSSCP) production within the Poaceae (grass) family. The results of detrended correspondence analysis show that grass subfamilies, tribes, and genera in this region can be differentiated through phytolith assemblages, and that these assemblages reflect the environmental conditions associated with various grass taxa. The developed detailed classification system and examination of co-occurrence patterns reduces redundancy of phytolith morphotypes across subfamilies, improving taxonomic and palaeoecological resolution of phytolith assemblages. Finally, based on the results of this study, a detailed scheme is presented for palaeoecological reconstructions in grassy ecosystems of northern Australia.

1. Introduction

Grassy ecosystems (grassland and savanna) cover nearly 75% of the Australian continent. These ecosystems range from the tropical grassy savannas of the far north, across the arid interior spinifex grasslands, to the southeastern temperate grasslands (Cheney and Sullivan, 2008). The distribution and composition of these ecosystems reflects biogeographic patterns of grass lineages (Lehmann et al., 2019; Bryceson et al., 2023), as well as contemporary environmental conditions including precipitation, moisture availability, soil properties and fire (Ehleringer, 2005; Edwards and Smith, 2010; Visser et al., 2012). However, little is known about the environmental and evolutionary history of Australia's grassy ecosystems, partly due to a lack of proxies that provide detailed resolution on grass communities (MacPhail and Hill, 2002). Further information about changes in grassy ecosystems through time may help to inform topics such as the ecological context of megafaunal decline and extinction (Bird et al., 2013; Llewelyn et al., 2021), modelling of human

arrival in and movement across the continent (Crabtree et al., 2021; Salles et al., 2024), the influence of Indigenous peoples on landscapes through fire management (Mariani et al., 2022; Bird et al., 2024), and the impacts of grassy weed invasion on ecosystem dynamics and fire regimes (Schlesinger et al., 2013; Setterfield et al., 2013).

Pollen and plant macrofossils have traditionally predominated as proxies for vegetation reconstructions in Australian palaeoecology (MacPhail and Hill, 2002). However, there is a clear spatial disparity in these records favouring the temperate south-east regions of the continent (MacPhail and Hill, 2002; Reeves et al., 2013). Very few pollen and macrofossil records have been recovered from Australia's arid zone (e. g., Singh, 1981; Boyd, 1990). Additionally, grass macrofossils are rare, and although pollen records are highly useful for discerning forest dynamics at fine taxonomic levels, they poorly represent grass dynamics due to uniform morphology across the Poaceae family (MacPhail and Hill, 2002). Further research into alternative palaeoecological proxies is thus needed to understand the environmental history and drivers of

change in Australia's grassy ecosystems.

An alternative proxy for reconstructing past grassy ecosystems are phytoliths, which are microscopic biogenic silica bodies formed in living plant tissues and deposited into underlying soils (Piperno, 2006; Strömberg et al., 2018). Patterns of silica accumulation in plant tissues are genetically determined along plant lineages, and thus patterns of phytolith production and morphology differ between plant taxa (Piperno, 2006). Plants produce a variety of phytolith morphotypes in their tissues (an issue known as multiplicity), including some morphotypes which are widely produced among plant taxa (an issue known as redundancy) (Piperno, 2006). The study of modern plant reference material is therefore necessary to understand patterns of phytolith production in local and regional vegetation communities (Strömberg et al., 2018). Unlike pollen and other proxies, phytoliths are highly robust due to their biogenic silica structure and can tolerate a wide range of environmental conditions (Strömberg et al., 2018). The development of phytolith analysis techniques worldwide has thus widened the range of depositional environments useful for palaeoecological research and has provided insight into taxa that do not preserve well in other records (e.g., Murungi and Bamford, 2020; Groff et al., 2022).

The application of phytolith analysis to Australian environments has been restricted by a lack of modern plant reference material (limited to Bowdery, 1998; Hart, 1997, 1990; Wallis, 2000, 2003; Parr and Watson, 2007), which is necessary for interpretation of fossil phytolith records. Furthermore, the limited existing reference material was described before standardisation of morphology through publication of the International Code for Phytolith Nomenclature 1.0 (Madella et al., 2005) and 2.0 (ICPT, 2019) further limiting its application. Although the spatial and botanical scope of published reference material highlights the applicability of phytolith analysis to Australian environments, a recent review by Turnbull et al. (2023) highlights numerous uncertainties and gaps surrounding phytolith production in Australian vegetation. Therefore, further studies of phytoliths from modern plants are necessary for the application of phytolith analysis to Australian sedimentary records.

The Poaceae (grass) and Cyperaceae (sedge) families are among the highest silica accumulating plant families that also produce diagnostic phytolith morphotypes (Piperno, 2006). The Cyperaceae produce a unique cone-shaped morphotype (also referred to as hat-shaped or papillar), with a pitted variation in the inflorescence that may be indicative of genera (Ollendorf, 1992; Murungi and Bamford, 2020). The Poaceae produce a wide variety of morphotypes indicative of subfamily, tribes, and even genera, known as the grass silica short cell phytoliths (GSSCP) (Piperno, 2006; ICPT, 2019). GSSCP are usually classified into seven main types: rondel, trapezoid, crenate, saddle, bilobate, cross, and polylobate (ICPT, 2019). It has long been accepted that Poaceae subfamilies produce different GSSCP morphotypes, such as, saddles in Chloridoideae, trapezoids in Pooideae, and crosses in Panicoideae (Piperno, 2006). However, some GSSCP (such as bilobates and rondels) are produced by many subfamilies, increasing redundancy in these categories. Recent studies have increasingly emphasised the use of detailed GSSCP classification schemes and multivariate morphospace analysis in phytolith research to reduce redundancy and improve taxonomic and palaeoecological resolution of grass phytoliths (Barboni and Bremond, 2009; Novello et al., 2012; Neumann et al., 2017; Bourel and Novello, 2020).

To bridge gaps in the knowledge and classification of Poaceae and Cyperaceae phytoliths in Australian environments, this study presents modern phytolith reference material for 49 grass and 4 sedge species from the grassy ecosystems of northern Australia. With it, a detailed classification scheme for GSSCP is developed from key grasses belonging to six subfamilies (Panicoideae, Chloridoideae, Aristidoideae, Arundinoideae, Oryzoideae, Micrairoideae) across the ecological gradient from the northern monsoonal grassy savannas to the arid interior grasslands of the Northern Territory, Australia. This data is analysed in a multivariate morphospace to examine taxonomic and environmental influences on production patterns. Finally, the potential relevance of these findings for palaeoecological reconstructions are discussed.

2. Environmental setting

The Northern Territory (NT) of Australia comprises the central northern region of the continent, between 129° - 138° E and 26° S, meeting the Timor and Arafura seas to the north at approximately 10° S (Fig. 1). The region is characterised by high mean annual temperatures, strong summer rainfall seasonality, and a strong north–south precipitation gradient, as a result of the Indo-Australian Summer Monsoon (IASM) system (Williams et al., 1996; Hutley et al., 2011; Ma et al., 2013) (Fig. 1). The far north of the NT experiences a tropical monsoon climate dominated by summer rainfall, gradually transitioning southwards into a semi-arid climate with low total rainfall as the influence of the IASM weakens (Hutley et al., 2011; Williams et al., 1996). Precipitation and lithology/soil texture act as predominant controls on ecosystem structure, composition, and distribution in the NT, driving strong latitudinal changes from north to south (Fig. 1) (Williams et al., 1996; Hutley et al., 2011; Ma et al., 2013).

Far north tropical landscapes are characterised largely by tropical Eucalypt open forest and woodlands (savannas) with a continuous, tallgrass understorey dominated by members of the Panicoideae subfamily, most notably *Sorghum, Themeda,* and *Heteropogon* species (Groves and Whalley, 2002; Cheney and Sullivan, 2008). The underlying soils are typically loamy with low clay content (Williams et al., 1996). The grassy layer may be dominated by *Triodia* species (Chloridoideae subfamily) in areas with nutrient-poor or rocky soils (Bowman et al., 2010). Other species from the Chloridoideae and Aristidoideae subfamilies replace the understorey as rainfall declines and clay content rises southwards, forming semi-arid open woodlands (Williams et al., 1996; Cheney and Sullivan, 2008; Bowman et al., 2010; Hutley et al., 2011). In some areas, semi-arid tussock grasslands (*Astrebla* species) are dominant. Tree cover declines and soil clay content peaks further south, with ecosystems fading into semi-arid hummock grasslands dominated by *Triodia* species (commonly known as spinifex) (Williams et al., 1996; Hutley et al., 2011). These grasses grow in circular mounds (hummocks), which may be interspersed by other semi-arid tussock grasses such as *Aristida, Enneapogon,* and *Sporobolous* species (Groves and Whalley, 2002; Cheney and Sullivan, 2008). These communities form a mosaic with patches of *Acacia* shrubland, which may have a tussock grass or bare understorey (Groves, 1994).

3. Material and methods

Grass specimens were primarily collected from around three lake sites in the NT: Girraween Lagoon, Lake Woods, and Lake Lewis (Fig. 1, Table 1). Further vegetation sampling was carried out across the regions surrounding each lake site. Remaining species of ecological and/or taxonomic interest were collected from other localities (Table 1) or sampled from either the John T. Waterhouse Herbarium at the University of New South Wales, or the Australian Tropical Herbarium at James Cook University, Cairns Nguma-bada campus. Information regarding taxonomic identification, vegetation communities, and other environmental factors were recorded at the time of collection. Identification of grass and sedge specimens to a species level was carried out with assistance and validation from the John T. Waterhouse Herbarium.

Phytolith extraction from plant material follows a dry-ashing method (Parr et al., 2001). Specimens were first sub-sampled by anatomical section (blade, culm, inflorescence, root) where available. Up to 3 g of species sampled in the field and 1 g of species sampled in herbariums was analysed. Samples were cleaned three times in an ultrasonic bath for 15 min with 5% sodium hexametaphosphate solution. Samples were rinsed and dried before being heated in a 450 °C furnace for 2 h to remove organic material. Remaining material was transferred to 50 cc tubes and treated with 10% HCl in 2 ml aliquots until the reaction
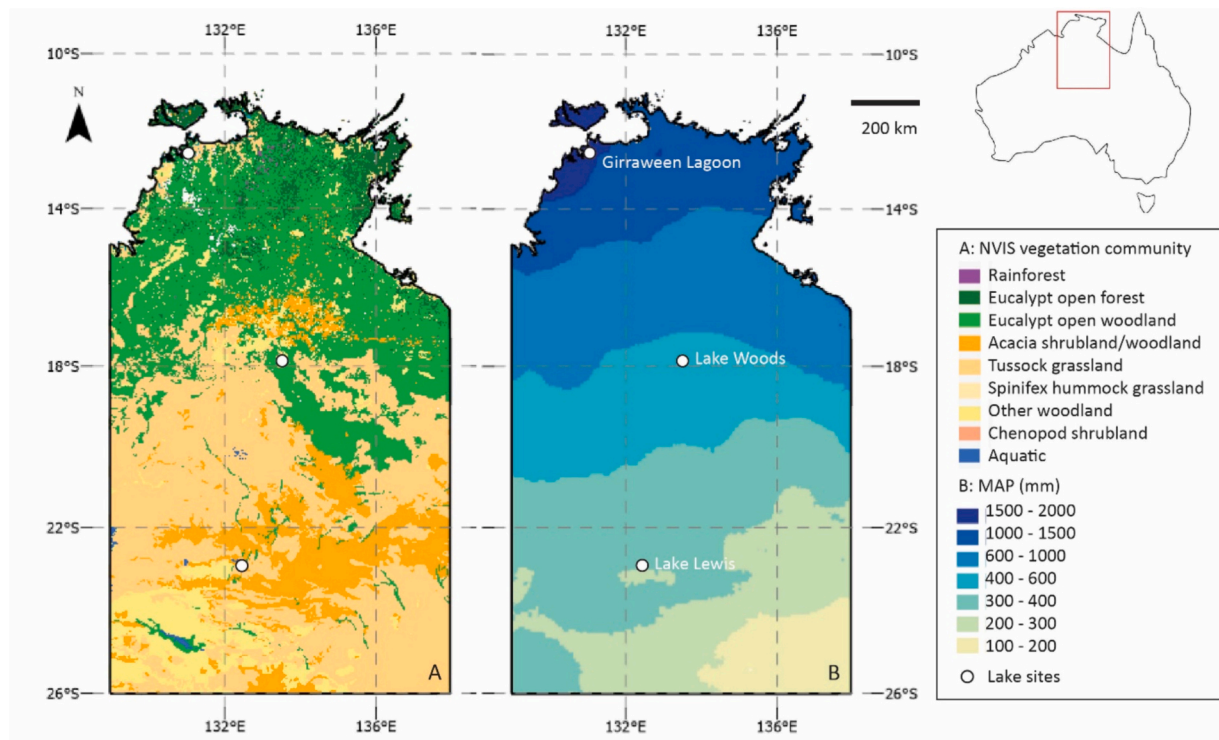
Fig. 1. Maps of the Northern Territory region of Australia. A: Major vegetation communities for the NT, modified from the National Vegetation Information System (NVIS) dataset. B: Mean Annual Precipitation (mm) values from 1991 to 2020 for the NT, from gridded rainfall data for the corresponding years from the Bureau of Meteorology (2023).

ceased. Samples were rinsed three times with deionised water before transfer with ethanol to small vials for storage. A total of 146 samples from 49 grass and 4 sedge species were sampled for analysis.

A small amount of each sub-sample was then mounted onto a glass slide and coverslip using Eukitt-UV as a medium. UV light was not applied to slides until they were stored, to allow rotation and examination of three-dimensional phytolith structure. Identification and counting of morphotypes was conducted at 400x magnification using an Olympus Bx51 light microscope. Each sample was counted to a minimum of 200 GSSCPs, followed by scanning of the slide to identify any rare morphotypes. Classification of non-GSSCP and major GSSCP morphotype classes follows the International Code for Phytolith Nomenclature 2.0 (ICPT, 2019). A detailed GSSCP morphotype classification scheme was developed using descriptive shape characteristics and quantitative measurements (see Section 4). GSSCP morphotype frequency per sample was calculated as the percent of each morphotype relative to the sum of all GSSCP counted in each sample. GSSCP morphotype frequency per species was calculated from the sum of all anatomical sub-samples from each specimen.

Taxonomic and environmental data for each grass species was compiled from relevant literature, including distribution (ALA, 2021), subfamily and tribe affiliations (Soreng et al., 2017), and photosynthetic pathway (Munroe et al., 2022). Environmental information recorded during specimen collection was used to categorise species vegetation community. Additional data for mean annual precipitation (MAP) and maximum and minimum mean annual temperatures (MAT) was compiled for each sampling location, using monthly records of the three years preceding sample collection from the closest available weather station (BOM, 2023).

Statistical analyses were carried out in RStudio on a matrix of species and GSSCP morphotype frequency (RStudio, 2022). Detrended correspondence analysis (DCA) was performed using the vegan package (Oksanen et al., 2022), with taxonomic and environmental factors introduced as passive variables to assess which factors may be influencing the dataset. ANOVA tests were used to evaluate the significance of precipitation and temperature gradients on the dataset. The dataset was then transformed to a presence/absence matrix for probabilistic co-occurrence analysis using the co-occur package (Griffith et al., 2016). This analysis compares the expected probability of co-occurrence in an independent dataset with observations of GSSCP morphotype co-occurrence in the dataset to produce the probability of GSSCP morphotypes co-occurring either significantly (at a < 0.01 threshold) more or less than expected. This data is used to examine whether GSSCP morphotypes are being produced together in the same taxa (positive co-occurrence) or by different taxa (negative co-occurrence).

4. GSSCP morphotype classification

Major GSSCP classes are described according to the ICPN 2.0 (ICPT, 2019), specifically the rondel, saddle, bilobate, cross, polylobate, and trapezoid categories. The first five categories were further separated into distinguishable subtypes, with naming conventions following those recommended in the ICPN 2.0. Each subtype is given a three-letter code corresponding to the GSSCP category (RON, SAD, BIL, CRO, POL, TRA), followed by a number representing the subtype. A drawing of each GSSCP subtype from top and transverse views is shown in Fig. 2, with corresponding descriptions in Table 2.

The identification of subtypes within each category primarily uses a range of descriptive shape characteristics of both two-dimensional and three-dimensional structures (Fig. 2). Two-dimensional structure refers to the planar view (IPS or OPS shape) structure. Quantitative measurements were also made of longest length and width of the IPS surface to constrain the size of each morphotype. Three-dimensional GSSCP structure is considered here as the shape of the top or inner periclinal surface (IPS) versus the base or outer periclinal surface (OPS) and side and end views, as defined in the ICPN 2.0 (ICPT, 2019).

Rondels are traditionally classified as GSSCP with an approximately circular or ovular two-dimensional shape in the ICPN 2.0 classification.

Table 1

Species, taxonomy, location, and herbarium voucher identifications for 49 grass and 4 sedge specimens collected from the Northern Territory, Australia.

Species	Family	Subfamily	Tribe/Subtribe	Site/Herbarium #
Alloteropsis semialata (R.Br.) Hitchc.	POACEAE	Panicoideae	Paniceae	Girraween Lagoon
Aristida capillifolia Henrard	POACEAE	Aristidoideae	Aristideae	Lake Lewis
Aristida contorta F. Muell.	POACEAE	Aristidoideae	Aristideae	Lake Lewis
Aristida holathera Domin	POACEAE	Aristidoideae	Aristideae	Lake Lewis
Aristida inaequiglumis Domin	POACEAE	Aristidoideae	Aristideae	Alice Springs
Aristida latifolia Domin	POACEAE	Aristidoideae	Aristideae	Yuendumu
Astrebla lappacea (Lindl.) Domin	POACEAE	Chloridoideae	Eleusininae	Fowlers Gap
Bothriochloa bladhii (Retz.) S.T.Blake	POACEAE	Panicoideae	Andropogoneae	Girraween Lagoon
Chrysopogon fallax S.T.Blake	POACEAE	Panicoideae	Andropogoneae	Herbarium no. UNSWDB 9165
Chrysopogon sp Trin.	POACEAE	Panicoideae	Andropogoneae	Girraween Lagoon
Cymbopogon ambiguus (Hack.) A.Camus	POACEAE	Panicoideae	Andropogoneae	Lake Lewis
Dichanthium sericeum (R.Br.) A.Camus	POACEAE	Panicoideae	Andropogoneae	Alice Springs
Digitaria brownii (Roem. and Schult.) Hughes	POACEAE	Panicoideae	Paniceae	Lake Lewis
Enneapogon pallidus (R.Br.) P.Beauv.	POACEAE	Chloridoideae	Cotteinae	Lake Woods
Enneapogon polyphyllus (Domin) N.T.Burb.	POACEAE	Chloridoideae	Cotteinae	Alice Springs
Enteropogon ramosus B.K.Simon	POACEAE	Chloridoideae	Eleusininae	Alice Springs
Eragrostis elongata (Willd.) J.Jacq.	POACEAE	Chloridoideae	Eragrostidinae	Lake Lewis
Eragrostis parviflora (R.Br.) Trin.	POACEAE	Chloridoideae	Eragrostidinae	Alice Springs
Eragrostis pergracilis S.T.Blake	POACEAE	Chloridoideae	Eragrostidinae	Lake Lewis
Eriachne burkittii Jansen	POACEAE	Micrairoideae	Eriachneae	Girraween Lagoon
Eriachne obtusa R.Br.	POACEAE	Micrairoideae	Eriachneae	Lake Woods
Eriachne sp R.Br.	POACEAE	Micrairoideae	Eriachneae	Yuendumu
Eriachne triseta Nees ex Steud.	POACEAE	Micrairoideae	Eriachneae	Girraween Lagoon
Eulalia aurea (Bory) Kunth	POACEAE	Panicoideae	Andropogoneae	Lake Lewis
Heteropogon contortus 1 (L.) P.Beauv. ex Roem. and Schult.	POACEAE	Panicoideae	Andropogoneae	Girraween Lagoon
Heteropogon contortus 2 (L.) P.Beauv. ex Roem. and Schult.	POACEAE	Panicoideae	Andropogoneae	First Horse Swamp
Heteropogon triticeus (R.Br.) Stapf ex Craib	POACEAE	Panicoideae	Andropogoneae	Girraween Lagoon
Iseilema vaginiflorum Domin	POACEAE	Panicoideae	Andropogoneae	Lake Woods
Oryza australiensis Domin	POACEAE	Oryzoideae	Oryzeae	Herbarium no. CNS 142438.1
Oryza meridionalis N.Q.Ng	POACEAE	Oryzoideae	Oryzeae	UNSWDB 11763
Panicum decompositum R.Br.	POACEAE	Panicoideae	Paniceae	Lake Eyre
Phragmites australis (Cav.) Trin. ex Steud	POACEAE	Arundinoideae	Moliniinae	Wollongong
Phragmites karka (Retz.) Trin. ex Steud.	POACEAE	Arundinoideae	Moliniinae	Herbarium no. CNS 151912
Schizachyrium fragile (R.Br.) A.Camus	POACEAE	Panicoideae	Andropogoneae	Lake Woods
Setaria sp P.Beauv.	POACEAE	Panicoideae	Paniceae	Girraween Lagoon
Setaria surgens Stapf	POACEAE	Panicoideae	Paniceae	Lake Woods
Sorghum intrans F.Muell. ex Benth.	POACEAE	Panicoideae	Andropogoneae	Girraween Lagoon
Sorghum plumosum (R.Br.) P.Beauv.	POACEAE	Panicoideae	Andropogoneae	Herbarium no. CNS 145190
Sporobolus actinocladus (F.Muell.) F.Muell.	POACEAE	Chloridoideae	Sporobolinae	Lake Lewis
Sporobolus australasicus Domin	POACEAE	Chloridoideae	Sporobolinae	Lake Woods
Sporobolus caroli Mez	POACEAE	Chloridoideae	Sporobolinae	Lake Lewis
Themeda triandra Forssk.	POACEAE	Panicoideae	Andropogoneae	Lake Lewis
Triodia basedowii E.Pritz.	POACEAE	Chloridoideae	Triodiinae	Herbarium no. UNSWDB 3822
Triodia bitextura Lazarides	POACEAE	Chloridoideae	Triodiinae	Katherine
Triodia pungens R.Br.	POACEAE	Chloridoideae	Triodiinae	Lake Lewis
Triodia sp 1 R.Br.	POACEAE	Chloridoideae	Triodiinae	Yuendumu
Triodia sp 2 R.Br.	POACEAE	Chloridoideae	Triodiinae	Lake Lewis
Triodia sp 3 R.Br.	POACEAE	Chloridoideae	Triodiinae	Lake Woods
Zygochloa paradoxa (R.Br.) S.T.Blake	POACEAE	Panicoideae	Paniceae	Herbarium no. UNSWDB 6904
Cyperus blakeanus K.L.Wilson	CYPERACEAE	NA	NA	Lake Lewis
Cyperus ixiocarpus F.Muell.	CYPERACEAE	NA	NA	Lake Lewis
Cyperus sp L.	CYPERACEAE	NA	NA	Girraween Lagoon
Scleria lingulata C.B.Clarke	CYPERACEAE	NA	NA	Katherine

Within this category there is high variation in three-dimensional shape and size, but generally the IPS and OPS faces are non-parallel (ICPT, 2019). Separation of rondel subtypes is hence by variation in two-dimensional and three-dimensional structure (see Fig. 2). Many rondel subtypes described here have an approximately circular or ovular planar view with a tall or tower three-dimensional structure, and either a plateaued top surface (RON-1, RON-2, RON-3), or keeled top surface (RON-4, RON-5). RON-8 variations have a varying planar view shape, from rounded edge squares to ovular forms, with a trapezoidal-like three-dimensional structure of varying relative height. RON-7 is a constricted form of the bilobate BIL-17, with a round or trapezoidal IPS shape (instead of bilobate). RON-6 is the only described rondel subtype with parallel IPS and OPS surfaces, with a reniform two-dimensional shape.

Saddles are traditionally classified as symmetrical GSSCP with two convex faces connected by two concave faces, with a concave three-dimensional structure. Traditional saddle subtypes are separated by length of convex and concave faces being either smaller or larger than

12 μm in length (SAD-1 - SAD-4); morphotypes SAD-1 and SAD-2 are typically described as squat saddles (Piperno, 2006) (see Fig. 2). One other saddle morphotype is described here (SAD-5), which has a tall three-dimensional shape instead of concave; this morphotype is often described as a tall or plateaued saddle (Piperno and Pearsall, 1998; Cordova and Scott, 2010; Cordova, 2013; ICPT, 2019).

Bilobates are traditionally classified as morphotypes with two lobes separated by a distinct shank in planar view. The exception to this is BIL-17 (unilobes), which describes all GSSCP with a shank and one lobe, being bilobates broken in half along the shank. Here, bilobates are divided into further subtypes (see Fig. 2) first by lobe end shape, which may be convex, concave, flat, scooped, pointed, or dissimilar (e.g., BIL-12, BIL-8, BIL-4, BIL-9, BIL-11, BIL-10). Further subtypes were differentiated by lobe width relative to shank (BIL-14, BIL-15, BIL-16), shank length and width (BIL-1, BIL-5, BIL-6, BIL-7, BIL-14, BIL-16), three-dimensional shape (BIL-2, BIL-3, BIL-11, BIL-12, BIL-13, BIL-18), and total length (BIL-14). BIL-18 appears as a bilobate encompassed by a

Fig. 2. Drawings of the 44 GSSCP subtypes identified across 49 grass species from the Northern Territory, Australia. Scale bars: 20 μm.

circular shape in planar view, with a bilobate-shaped IPS surface, and wide, multi-faceted three-dimensional structure.

Both cross and polylobate morphotypes can be considered along a morphological spectrum with bilobates (Fig. 2). Crosses are traditionally classified as morphotypes with four distinct lobes and mirror symmetry in planar view, which is expanded here to also include types with three lobes. These subtypes are differentiated hence by number of lobes (CRO-1 to CRO-3 vs CRO-4 to CRO-7), three-dimensional shape (CRO-2, CRO-5, CRO-6, CRO-7) and planes of symmetry (CRO-3, CRO-6, CRO-7). Polylobates are classified as morphotypes with two end lobes separated by a shank, with one or more additional lobes along the shank. Subtypes were further differentiated based on lobe end shape (POL-2, POL-3, POL-5), three-dimensional structure (POL-2), and total length (POL-5).

5. Results

5.1. Morphotype production

5.1.1. Sedges and grasses: Non-GSSCP morphotypes

Three species from the genus *Cyperus* and one species from *Scleria* were examined from the Cyperaceae family. A range of morphotypes were observed, including the diagnostic conical papillar type with psilate (Plate I 56, 57) or scrobiculate (Plate I 58) ornamentation, as well as acute bulbosus, flabellate bulliform, elongate, blocky, and annular/helical tracheary (Plate I 49–55, 59–62). Scrobiculate papillar morphotypes were only observed in *Cyperus* inflorescence samples (Supplementary Material Fig. S1).

49 grass species were examined for their silica content, consisting of

Table 2

Descriptions of the 44 GSSCP morphotypes identified in 47 grass species collected from the Northern Territory, Australia.

Code	Name	2-D structure	3-D structure	Size
RON-1	Tapered tower rondel	Circular	Tapering conical	5–10 μm wide, ≤25 μm tall
RON-2	Tall tower rondel	Rounded or ovular	Conical with truncated top	5–10 μm wide, 8–15 μm tall
RON-3	Wide tower rondel	Ovular or saddle-like	Wide conical with truncated top	8–15 μm wide, 8–18 μm tall
RON-4	Ovular keeled rondel	Ovular or irregular	Wide conical with keeled top	8–15 μm wide, 8–18 μm tall
RON-5	Circular keeled rondel	Circular	Pyramidal with keeled top	5–10 μm wide and tall
RON-6	Reniform rondel	Reniform	Flattened trapezoid	8–18 μm wide
RON-7	Rondel on base	Trapezoidal or circular shape surrounded by sheet	Facetate concave polyhedral	8–18 μm wide and tall
RON-8a	Trapezoidal rondel	Trapezoidal or ovular	Cylindrical with flat top	8–18 μm wide and tall
RON-8b	Tall trapezoidal rondel	Trapezoidal or ovular	Cylindrical with flat top	8–18 μm wide, 18–24 μm tall
TRA-1	Trapezoidal	Trapezoidal	Flat trapezoidal	8–15 μm
SAD-1	Squat saddle	Convex edges equal to or longer than concave edges	Convex	<12 μm long and wide
SAD-2	Squat saddle	Concave edges longer than convex edges.	Convex	<12 μm wide, >12 μm long
SAD-3	Wide saddle	Concave edges equal to or longer than convex edges.	Convex	>12 μm long and wide
SAD-4	Wide saddle	Convex edges longer than concave edges.	Convex	<12 μm long, >12 μm wide
SAD-5	Tall saddle	Concave edges equal to or longer than convex edges.	Conical with truncated top	8–15 μm long, <12 μm wide
BIL-1	Small bilobate	Small truncated lobes with a constricted shank	Convex	8–18 μm long
BIL-2	Tall bilobate	Small flat or convex lobes with constricted shank	Conical with truncated top	8–18 μm long
BIL-3	Tall bilobate	Flat or convex lobes with short, wide shank	Conical with truncated top	15–26 μm long
BIL-4	Flat lobe bilobate	Flat lobes with short or medium, wide shank	Convex	10–26 μm long
BIL-5	Long shank bilobate	Flat lobes with long, wide shank	Convex	10–26 μm long
BIL-6	Thin shank bilobate	Flat lobes with long, thin shank	Convex	10–26 μm long
BIL-7	Thin shank bilobate	Flat or convex lobes with short, thin shank	Convex	10–26 μm long
BIL-8	Concave bilobate	Concave lobes with short or medium, wide shank	Convex	10–26 μm long
BIL-9	Scooped bilobate	Scooped lobes with short or medium, wide shank	Convex	10–26 μm long
BIL-10	Half concave bilobate	One concave lobe and one flat lobe with short or medium, wide shank	Convex	10–26 μm long
BIL-11	Pointed bilobate	Pointed lobes with short, wide shank	Trapezoidal	10–26 μm long
BIL-12	Trapezoidal bilobate	Convex lobes with short, wide shank	Trapezoidal	10–26 μm long
BIL-13	Unequal bilobate	Convex lobes of unequal size, with constricted shank	Trapezoidal	10–18 μm long
BIL-14	Long narrow bilobate	Flat or convex lobes with long, thick shank	Convex	18–36 μm long
BIL-15	Wide bilobate	Flat, wide lobes with short or medium, thick shank	Convex	10–26 μm long
BIL-16	Thin shank wide bilobate	Flat, wide lobes with short or medium, thin shank	Convex	10–26 μm long
BIL-17	Unilobe	Bilobate broken along shank	Convex	≤18 μm long
BIL-18	Bilobate on base	Bilobate shape on circular base	Facetated concave polyhedral	10–26 μm long
CRO-1	Three-lobe cross	3 symmetrical lobes	Convex	10–18 μm long
CRO-2	Three-lobe tall cross	2 symmetrical lobes and one larger lobe	Convex	10–18 μm long
CRO-3	Four-lobe flat cross	4 symmetrical lobes or two pairs of symmetrical lobes	Convex	8–26 μm long
CRO-4	Four-lobe tall cross	4 symmetrical lobes	Conical with truncated top	8–15 μm long, 12–18 μm tall
CRO-5	Four-lobe tall cross	2 pairs of symmetrical lobes	Conical with truncated top	12–26 μm long, 12–17 μm tall
CRO-6	Four-lobe keeled cross	2 pairs of symmetrical lobes	Pyramidal with keeled top	10–26 μm long, 12–17 μm tall
POL-1	Keeled polylobate	At least three convex lobes	Pyramidal with keeled top	10–26 μm long, 12–17 μm tall
POL-2	Convex polylobate	≥3 convex lobes	Convex	10–26 μm long
POL-3	Flat polylobate	≥3 flat lobes	Convex	10–26 μm long
POL-4	Square polylobate	≥3 square lobes	Convex	10–26 μm long
POL-5	Long narrow polylobate	≥3 flat or convex lobes with long shank	Convex	≥26 μm long

25 genera across six subfamilies: Panicoideae, Chloridoideae, Aristidoideae, Micrairoideae, Arundinoideae, Oryzoideae. Non-GSSCP morphotypes were recovered from all 137 grass samples, with varying abundance across samples (Supplementary Material Fig. S1). The most common phytoliths were elongate entire, acute bulbosus, and blocky morphotypes (Plate I 49, 54, 55). Some anatomical differences in production were observed, such as a wider range and abundance of elongate morphotypes in inflorescence samples (Supplementary Material Fig. S1). Two further distinct forms of bulliform morphotypes were also observed: scooped blocky and flabellate bulliform morphotypes, and rounded, large flabellate bulliforms (Plate I 59, 60).

5.1.2. Grasses: GSSCP morphotypes

GSSCP morphotypes were recovered from 129 grass samples, with no GSSCP recovered from the eight root samples (Plate I 1–48, Fig. 3). The most common GSSCP morphotype was BIL-4, which was frequently

Plate I. Phytolith morphotypes extracted from grass and sedge species of the Northern Territory, Australia (All scale bars: 20 μm). Grass silica short cell phytoliths 1–48. 1: RON-1; 2: RON-2; 3: RON-3; 4: RON-4; 5: RON-5; 6: RON-6; 7: RON-7; 8, 9: RON-8a; 10: RON-8b; 11: TRA-1; 12: SAD-1; 13: SAD-2; 14: SAD-3; 15: SAD-4; 16, 17: SAD-5; 18: BIL-1; 19: BIL-2; 20: BIL-3; 21: BIL-4; 22: BIL-5; 23: BIL-6; 24: BIL-7; 25: BIL-8; 26: BIL-9; 27: BIL-10; 28: BIL-11; 29: BIL-12; 30: BIL-13; 31, 32: BIL-15; 33: BIL-16; 34: BIL-14; 35: BIL-17; 36, 37: BIL-18; 38: CRO-1; 39: CRO-2; 40: CRO-3; 41: CRO-4; 42: CRO-5; 43: CRO-6; 44: POL-1; 45: POL-2; 46: POL-3; 47: POL-4; 48: POL-5; 49: Elongate psilate; 50: Elongate dentate; 51: Elongate dendritic; 52: Elongate bulbous; 53: Elongate sinuate; 54: Acute bulbosus; 55: Blocky; 56, 57: Psilate papillar; 58: Scrobiculate papillar (achene); 59: Flabellate bulliform; 60: Scooped flabellate bulliform; 61: Scooped bulliform; 62: Annular/helical tracheary.
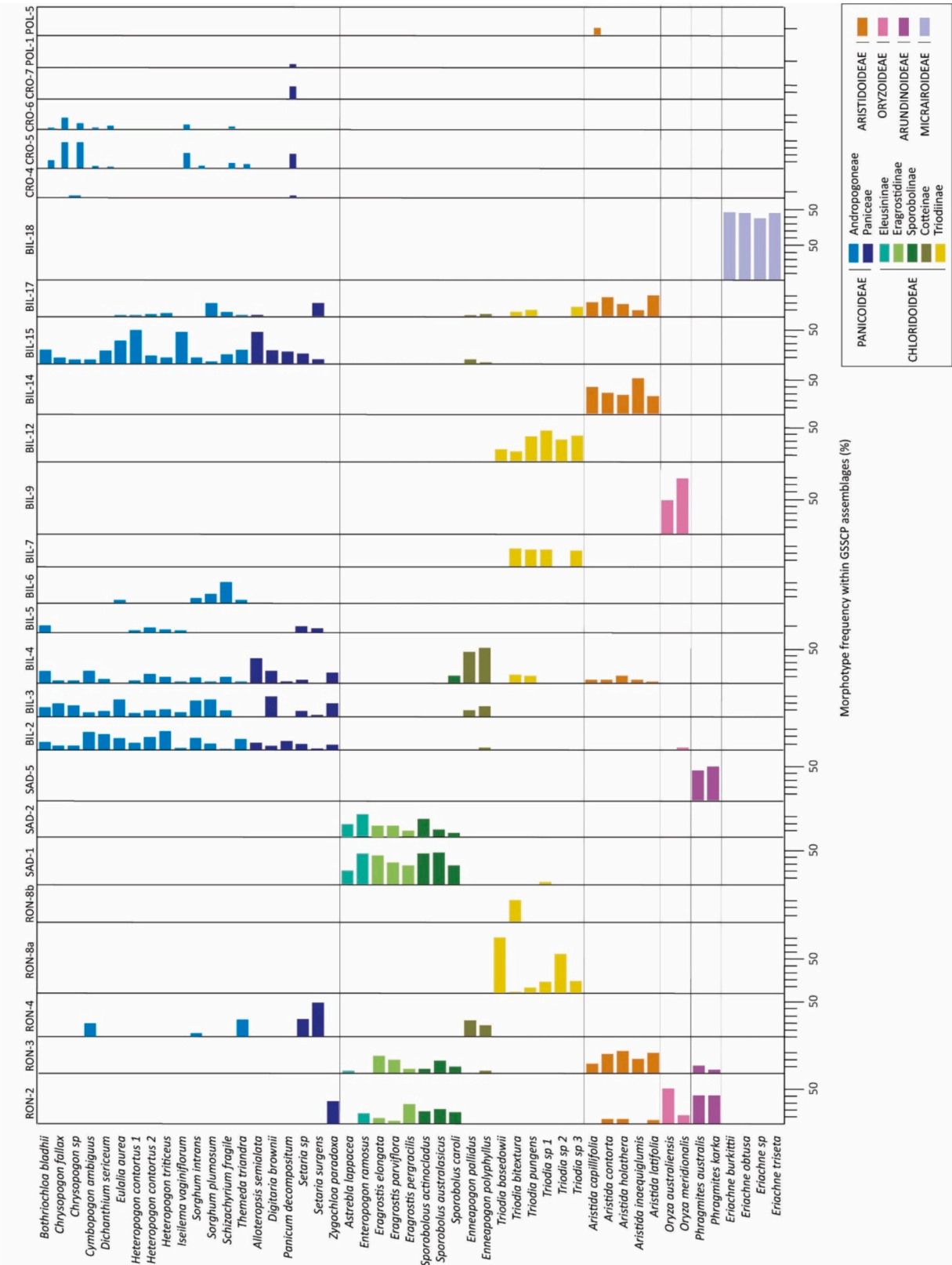
Fig. 3. Frequency (%) of common and/or specific GSSCP morphotypes within the total GSSCP assemblage for each species, across all 49 grass species from the Northern Territory, Australia.

observed in 27 species across three subfamilies (Fig. 3). Other common and widespread morphotypes were BIL-2, BIL-3, BIL-13, BIL-15, BIL-18, RON-2, and RON-3. 14 morphotypes were found in a limited number of species but were often abundant within these: RON-8a, SAD-1, SAD-2, SAD-5, BIL-6, BIL-9, BIL-14, BIL-18, CRO-4, CRO-5, CRO-6, CRO-7, POL-1, POL-5 (Fig. 3). 10 further morphotypes were widely observed across samples, but only in low (<10%) frequencies: RON-1, RON-5, RON-6, BIL-10, BIL-11, BIL-16, CRO-1, CRO-4, POL-2, and POL-3 (Fig. 3). A full representation of GSSCP production across all 137 anatomical specimens can be found in the Supplementary Material (Fig. S2)

5.2. Statistical analysis

5.2.1. Correspondence analysis

Non-GSSCP morphotypes were excluded from statistical analysis due to their redundancy within the Poaceae and Cyperaceae families (Piperno, 2006). Detrended Correspondence Analysis (DCA) was first carried out on a matrix of species and GSSCP morphotype frequency. The resulting ordination diagram (Supplementary Material Fig. S3) features a strong positive skew. These outlying points belong to *Eriachne* species and corresponding morphotypes, which overcontribute to the inertia of axis 1. Due to this, these species were removed from the matrix and the ordination repeated.

The subsequent DCA with *Eriachne* species removed features a spread of data across the axes, with no overcontributing points (Fig. 4). The first axis explains 12.6% of variation, the second axis 12.2%, the third axis 6.2%, and the fourth axis only 3.9%; axes 3 and 4 were disregarded due to low eigenvalues.

The dataset was then grouped by taxonomic affiliation using ordination hulls (Fig. 4). Panicoideae and Chloridoideae subfamilies are clearly differentiated along axis 1 (aside from the Cotteinae subtribe), and Aristidoideae is alone in the middle. The Paniceae and Andropogoneae tribes (Panicoideae) occupy overlapping areas on the negative side of axis 1 along with the Cotteinae subtribe (Chloridoideae), while the Eleusininae, Eragrostidinae, and Sporobolinae subtribes (Chloridoideae) occupy intersecting areas on the positive side of axis 1. The Triodiinae subtribe (Chloridoideae) is separated from the Panicoideae

subfamily along axis 2, on the positive side of the axis. Although these taxonomic groups can be clearly distinguished in the ordination, the distances between them are not directly comparable in Chi-square space.

Environmental factors were plotted on the ordination as hulls to assess their influence on the dataset. Vegetation community categories produce clear ordination groups along the axes (Fig. 5). Fitting of precipitation and temperature values as passive variables on the ordination shows a clear correlation between MAP and axis 2, while maximum MAT is correlated with the negative values of axis 1 and 2.

5.2.2. Analysis of morphotype relationships

Probabilistic co-occurrence analysis was performed on a transformed presence-absence matrix to assess relationships between morphotypes (Fig. 6). 990 morphotype pairings were analysed to produce a probability of co-occurring more or less than expected (compared to independent data), using a 0.01 threshold of significance. 358 pairings were found to have an expected co-occurrence of less than once and were removed. 60% of the analysed pairings were classified as random, with another 17% of pairings found to significantly co-occur (positively or negatively) in more than one species.

The morphotypes that most often co-occur (positively or negatively) were BIL-2, BIL-3, and BIL-15. These morphotypes were found to co-occur more than expected with each other, as well as a range of other morphotypes (Fig. 6). Additionally, BIL-2, BIL-3, and BIL-15 were also found to co-occur less than expected with RON-2 and RON-3. RON-2 and RON-3 positively co-occur with SAD-1, SAD-2, and SAD-4, while RON-3 also positively co-occurs with BIL-14. SAD-1, SAD-2, SAD-3, and SAD-4 all positively co-occur with each other, while SAD-1 also positively co-occurs with RON-8a, BIL-7 and BIL-12. SAD-1 also negatively co-occurs with BIL-15 and BIL-4.

6. Discussion

6.1. Cyperaceae family

The Cyperaceae family is represented in this study by four species across two genera, *Cyperus* and *Scleria*. The examination of four species provides only a limited view of the morphological variation among
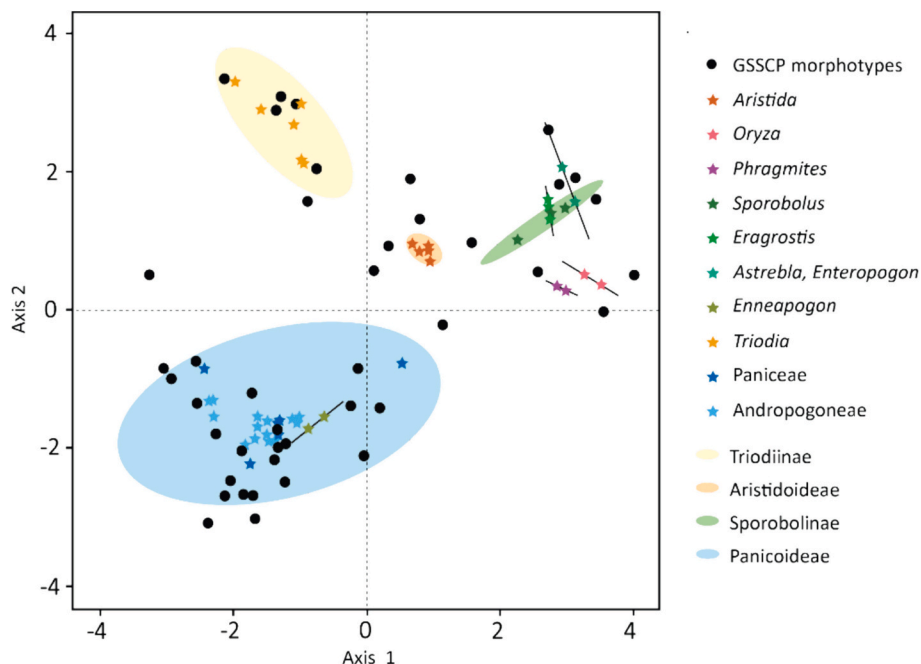

Fig. 4. Detrended correspondence analysis (DCA) of 45 grass species and 44 GSSCP morphotypes, axes 1 (12.6% of variation) and 2 (12.2% of variation). Markers show taxonomic affliations.
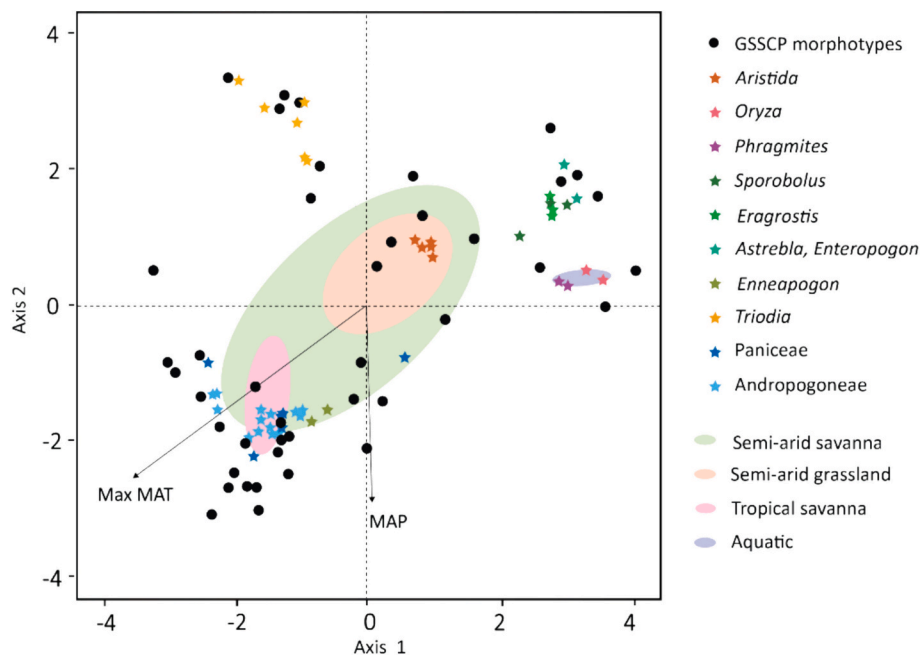
Fig. 5. DCA of 45 grass species and 44 GSSCP morphotypes, axes 1 (12.6% of variation) and 2 (12.2% of variation). Markers show taxonomic affiliations and environmental conditions where specimens were collected.
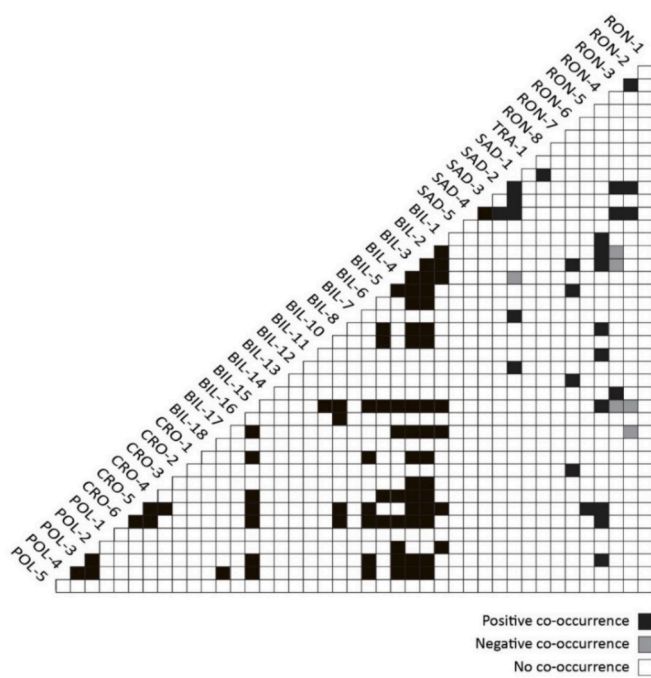

Fig. 6. Heat map of probabilistic co-occurrence between the 44 GSSCP morphotypes, using a presence-absence matrix of species and morphotypes across all 49 grass species.

sedge phytoliths, and therefore this study does not aim to discern taxonomic patterns within the family. These species produced a range of morphotypes that are redundant across both the Poaceae and Cyperaceae subfamilies, including flabellate bulliform, blocky, elongate, stomata phytoliths (Supplementary Material Fig. S2) (Piperno, 2006).

The psilate papillar morphotype (Plate I 56, 57) was observed in all sedge samples (Supplementary Material Fig. S2); this morphotype is widely accepted as a marker for the Cyperaceae family (Ollendorf, 1992; Piperno, 2006; Murungi and Bamford, 2020). Also observed in *Cyperus*

inflorescence samples were scrobiculate papillar morphotypes (Plate I 58). These morphotypes originate from the sedge fruit (achene). Some studies have suggested that sedge genera can be separated by morphological characteristics of achene papillar phytoliths (Piperno, 1989; Ollendorf, 1992), such as base shape, apex shape, and ornamentation. However, more recent studies suggest the need for revision of morphological criteria for this differentiation (Murungi and Bamford, 2020; Stevanato et al., 2019). Therefore, we propose psilate papillar as a general indicator of the Cyperaceae family, and scrobiculate papillar as a general indicator of Cyperaceae inflorescence. Future detailed studies of this family may better discern taxonomic patterns of production and improve palaeoecological resolution in this region.

6.2. Poaceae subfamilies

6.2.1. Panicoideae subfamily

The Panicoideae subfamily is represented in this study by 19 species across two tribes (Andropogoneae and Paniceae) and features the highest variation in phytolith morphotypes among the grass subfamilies examined (Fig. 3). Members produce a large diversity of GSSCP morphotypes, most importantly four lobed crosses (CRO-4 to 7) and wide lobe bilobates (BIL-15). While the four-lobed crosses are exclusive to this family, wide bilobates are produced in low frequencies by some members of the Chloridoideae; however, the abundance of this morphotype within the subfamily make it characteristic of the Panicoideae. Wide bilobates are widely associated with the Panicoideae in studies of African grasses, equivalent to 10-K and 10-W of Cordova (2013), BF/ML/LS and BF/ML/SS of Neumann et al. (2017), and Bi-3 of Novello et al. (2012). It is therefore proposed that morphotypes BIL-15, CRO-4, CRO-5, CRO-6, and CRO-7 may be used as markers of the Panicoideae subfamily in northern Australia (see Section 6.4).

Tall bilobates (BIL-2, BIL-3) are often considered to be widely produced across subfamilies (Neumann et al., 2017; Novello et al., 2012; Cordova, 2013), but co-occurrence data suggests that their production is more nuanced than previously considered (Fig. 6). Tall bilobates are found in all Panicoideae species and are particularly abundant in culm and inflorescence samples (Fig. 3; Supplementary Material Fig. S2). These morphotypes positively co-occur with BIL-15 in most species in

which they are present, but negatively co-occur with tall rondels (RON-2 and RON-3), which are not found in the Panicoideae (Fig. 6). BIL-2 and BIL-3 further positively co-occur with a range of other morphotypes common across the Panicoideae subfamily, including RON-4, CRO-5, CRO-6 (Fig. 6). This indicates that tall bilobates are usually produced by Panicoid grasses, and that they are being produced in the culm and inflorescence instead of the tall rondels found in other subfamilies. Keeled rondels (RON-4) are also abundant in the culm and inflorescence of some Panicoid grasses, and co-occur with BIL-2, BIL-3, and BIL-15 (Fig. 3; Supplementary Material Fig. S2). However, this morphotype also occurs in the Chloridoideae genus *Enneapogon*, making its taxonomic resolution unclear. Therefore, BIL-2 and BIL-3 may be used as an indicator of the subfamily when co-occurring with markers BIL-15, CRO-4, CRO-5, or CRO-6.

Contrary to other studies worldwide (Neumann et al., 2017; Cordova and Scott, 2010; Cordova, 2013; Piperno and Pearsall, 1998), polylobates do not appear to be closely associated with the Panicoideae species analysed here. Only morphotype POL-1 is produced within the Panicoideae subfamily, while morphotypes POL-2, POL-3, and POL-4 were also found in Chloridoideae and Micrairoideae species (Fig. 3). POL-4 morphotypes are highly abundant in a few Panicoideae species (*Dichanthium sericeum, Sorghum* species), and significantly positively co-occur with BIL-15, BIL-2, and BIL-3 (Fig. 3, Fig. 6). Therefore, abundance and co-occurrence of this morphotype with subfamily markers may further indicate Panicoid grasses. However, the occurrence of polylobate morphotypes alone cannot be considered representative of the Panicoideae in this region. The use of assemblage composition and frequency data in this way may help to reduce taxonomic uncertainties and redundancy associated with the high inter-species variability of Panicoideae grasses.

Tribes within the Panicoideae cannot be distinguished by their phytolith assemblages (Fig. 4). The assemblage composition of Andropogoneae and Paniceae grasses is generally similar, with high frequencies of wide bilobates and four-lobe crosses, and the tribes occupying overlapping areas of the DCA (Fig. 4). Notably, flat lobe, thin-shanked bilobates (BIL-6) were observed only in Andropogoneae species. However, some genera produce distinct assemblages that may reflect phylogeny (Fig. 3). *Zygochloa paradoxa* produces abundant tall tower rondels (RON-1 and RON-2), which may reflect the unclear evolutionary history and unusual physical structures of this genera (Novello et al., 2012). *Chrysopogon* species produce particularly abundant tall four-lobe crosses (CRO-5, CRO-6); this genus also has unclear phylogeny, placed within *incertae sedis* status by Soreng et al. (2017). *Panicum decompositum* also produces abundant crosses, including exclusive keeled crosses and polylobates (CRO-7, POL-1). Previous studies note high variation in GSSCP morphotypes across this genus, including the presence of unusual bilobate morphotypes (Fahmy, 2008; Novello and Barboni, 2015). Studies of further species are needed to discern the taxonomic significance of these morphotypes.

6.2.2. Chloridoideae subfamily, subtribes Eleusininae, Eragrostidinae, Sporobolinae

The Chloridoideae subfamily is represented in this study by five subtribes, which are presented here as three subgroups. Together, the Eleusininae, Eragrostidinae, and Sporobolinae subtribes are represented by seven grass species. Squat saddles (SAD-1 and SAD-2) are exclusively present in species of the Chloridoideae subfamily, and are particularly abundant in members of the Eleusininae, Eragrostidinae, and Sporobolinae tribes. This morphotype is widely recognised in phytolith studies as typical of Chloridoideae grasses (Piperno, 2006; Novello et al., 2012; Neumann et al., 2017; Cordova and Scott, 2010; Cordova, 2013; Barboni and Bremond, 2009) and thus SAD-1 and SAD-2 can be used as markers for the subfamily (see Section 6.4).

Tower rondels (RON-2 and RON-3) are also abundant in the Eragrostinidae and Sporobolinae subtribes, particularly in the culm and inflorescence (Fig. 3; Supplementary Material Fig. S2). Tall tower

rondels (RON-2) morphotypes positively co-occur with SAD-1, SAD-2, and SAD-4, and negatively co-occur with BIL-2 and BIL-3 (Fig. 6). This suggests that tall tower rondels are being produced in the culm and inflorescence of Chloridoideae grasses, instead of the tall bilobates found in the Panicoideae. However, RON-2 morphotypes are also abundant in the culm and inflorescence of *Oryza* (Oryzoideae) and *Phragmites* (Arundinoideae) species, limiting their taxonomic resolution within assemblages. Tower rondels are less abundant in Eleusininae species, which feature abundant wide saddles (SAD-3, SAD-4). These three subtribes occupy intersecting areas of the space in the ordination (Fig. 4), but it is unlikely that these tribes can be differentiated in phytolith assemblages.

6.2.3. Chloridoideae subfamily, subtribe Cotteinae

The Cotteinae subtribe is represented by two *Enneapogon* species, which contain dissimilar assemblages to other Chloridoideae grasses (Fig. 4). These species do not produce typical squat saddles, and are instead dominated by bilobate morphotypes, particularly BIL-4 (Fig. 3). The production of bilobate assemblages in this subfamily is described in previous studies (Barboni and Bremond, 2009; Novello and Barboni, 2015). This subtribe shows most similarity to the Panicoideae subfamily, producing wide bilobates (BIL-15) in low frequencies, and abundant long keeled rondels (RON-4) in culm and inflorescence samples. Accordingly, this subtribe occupies overlapping space with the Panicoideae subtribes in the DCA biplot (Fig. 4). However, assemblages from this subtribe can be distinguished from the Panicoideae by an absence of four-lobed cross morphotypes.

6.2.4. Chloridoideae, subtribe Triodiinae

The Triodiinae subtribe is represented here by six species of the genus *Triodia,* which is the only genus within this subtribe (Soreng et al., 2017). Only three of these specimens were identified to a species level, limiting examination of taxonomic variability within the subtribe. The Triodiinae subtribe shows significant departure from typical Chloridoideae production patterns. Although *Triodia* species produce characteristic squat saddles (SAD-1) as well as wide saddles (SAD-3, SAD-4), these morphotypes are not abundant in any samples examined (Fig. 3; Supplementary Material Fig. S2). There is also high morphological variability in GSSCP across the genus, which was previously noted by Bowdery (1998). This genus produces multiple morphotypes that were not observed in other species, and accordingly occupies a distinct space in the DCA biplot (Fig. 4). Because of this high morphotype variability, consideration of assemblage composition and frequency data is recommended.

The species *T. basedowii* and *Triodia* species 2 are dominated by trapezoidal rondel (RON-8a) morphotypes, which are also found in low abundances in all *Triodia* samples examined (Fig. 3; Supplementary Material Fig. S2). A variation of this morphotype with a taller relative height was also observed in the culm of *T. bitextura.* This morphotype was not observed in any other species studied, and was previously described by Wallis (2000, 2003) as a spheroidal grass phytolith. Wallis (2000, 2003) attributes this morphotype as a marker for the genus *Triodia,* which is supported by this study. However, this morphotype was not common in all *Triodia* species examined, and therefore it may not be a reliable sole indicator. Although only two morphological subtypes are classified here (by three-dimensional structure, see Fig. 2), high morphological variability in two-dimensional structure (planar view) of this morphotype was also observed. Thus, further studies into morphological diversity and production across the genus may help to further resolve its taxonomic and environmental significance.

Other species of this genus produced mainly bilobate morphotypes. *T. pungens, T. bitextura, Triodia* species 1, and *Triodia* species 3 are dominated by round lobe trapezoidal bilobates (BIL-12) and flat or convex lobed bilobates with thin, short shanks (BIL-7) (Fig. 3). Both of these morphotypes were also observed in the genus by Wallis (2000, 2003). Round lobe trapezoidal bilobates were not observed in any other

species, although trapezoidal bilobates with different lobe shapes (BIL-11) were found in other subfamilies (Fig. 3). Trapezoidal (or tabular, trapeziform) bilobates are generally considered representative of the Pooideae Stipeae tribe (Cordova and Scott, 2010; Cordova, 2013; Barboni and Bremond, 2009), so the taxonomic association of this morphotype is unclear. Neumann et al. (2017) additionally reports this morphotype to be representative of the Panicoideae subfamily in west Africa, highlighting the importance of regional phytolith reference collections. Comparison with phytolith assemblages from the genus *Austrostipa* (previously *Stipa*) may clarify the production of this morphotype in Australian environments.

Bilobates with short, very thin shanks were also not observed in other species, but show high morphological similarity with bilobates with long, thin shanks (BIL-6) which are found in the Panicoideae subfamily. Due to this similarity, these morphotypes may be misidentified in assemblages. Morphometric studies of GSSCP, particularly bilobate morphotypes, may help to improve the discrimination and palaeoecological resolution of these morphotypes.

6.2.5. Aristidoideae subfamily, genus Aristida

The Aristidoideae subfamily is represented in this study by five *Aristida* species. Bilobates with narrow, convex or flat lobes and very long shanks (BIL-14) are exclusively present and abundant in *Aristida* species (Fig. 3). This morphotype is equivalent to the Aristidoid bilobate of Piperno (2006), bilobates 10-A, 10-B and 10-C of Cordova (2013) morphotype BC(F)/VLL/VLS of Neumann et al. (2017), and Bi-15 of Novello et al. (2012). Also exclusive to *Aristida* species are long polylobates with narrow, convex lobes (POL-5), which were only observed in *A. capillifolia,* and are likely a variation of BIL-14 (Fig. 3). These bilobate and polylobate morphotypes can be used as indicators for the genus *Aristida* (see Section 6.4).

Other morphotypes common in this genus are unilobes (BIL-17) and wide tower rondels (RON-3). The high frequency of unilobes is most likely due to breaking of the fragile long shanks of BIL-14. It is difficult to identify the origin of unilobes due to a loss of identifiable characteristics (e.g., shank thickness, length). Wide tower rondels (RON-3) are particularly abundant in the culm and inflorescence of *Aristida* species, although they are also observed in Chloridoideae and Arundinoideae members (Fig. 3; Supplementary Material Fig. S2). This morphotype significantly positively co-occurs with BIL-14, as well as with tall tower (RON-2), and squat saddle (SAD-1) morphotypes (Fig. 6). This suggests that wide tower rondels are being produced in the culm and inflorescence of both Chloridoideae and *Aristida* grasses, but not by Panicoid grasses. High abundance of BIL-17 may indicate the presence of *Aristida* species, only when co-occurring with BIL-14. However, RON-3 cannot be used as an indicator of *Aristida* due to similar production patterns of the Aristidoideae and Chloridoideae subfamilies (ALA, 2021).

6.2.6. Micrairoideae subfamily, genus Eriachne

The Micrairoideae subfamily is represented in this study only by four *Eriachne* species. This genus has a unique evolutionary history among Australian grasses, evolving in situ rather than migrating from southeast Asia (Bryceson et al., 2023). Accordingly, this genus produces highly unique phytolith assemblages consisting almost solely of exclusive morphotypes; this led to overcontribution of these points to the first DCA ordination (Supplementary Material Fig. S3). Bilobates with wide, concave bases (BIL-18) and constricted variations (RON-7) are exclusive to this genus, and were previously described as bilobes on base by Wallis (2000, 2003) and (Bowdery, 1998), due to their planar view structure (Fig. 2). Because of the unique evolutionary history of this genus, this morphotype cannot be considered representative of the Eriachneae tribe (also containing *Pheidochloa* species) or Micrairoideae subfamily until examination of other species is conducted. However, the morphotypes BIL-18 and RON-7 can be used as markers of the genus *Eriachne* (see Section 6.4).

6.2.7. Oryzoideae subfamily, genus Oryza

The Oryzoideae subfamily is presented in this study only by the genus *Oryza,* which is the only native genus of this subfamily occurring in the NT (ALA, 2021). Bilobates with scooped lobes (BIL-9) are exclusively present and abundant in the two species of *Oryza* (Fig. 3, Plate I 26, Supplementary Material Fig. S2). BIL-9 is equivalent to Bsco/ML/SS of Neumann et al. (2017) and lobates 5, 6, and 11 of Lu and Liu (2003). Scooped bilobates have been identified in other genera within the Oryzeae tribe (e.g., *Zizania, Leersia*) by Yost and Blinnikov (2011) and Lu and Liu (2003), and therefore are a marker of the Oryzeae tribe (see Section 6.4).

Oryza species also produced distinctive non-GSSCP morphotypes. Scooped bulliform morphotypes were abundant in leaf and particularly inflorescence samples (Supplementary Material Fig. S1; Plate I 60, 61). Scooped bulliforms have been observed in other Oryzeae genera and are widely accepted as a marker for the Oryzeae tribe (Pearsall et al., 1995; Yost and Blinnikov, 2011; Lu and Liu, 2003; Chen et al., 2020). Both scooped bilobates and scooped bulliforms were previously identified from studies of *Oryza* in Kakadu National Park, Northern Territory, by Fujiwara et al. (1985). These morphotypes have been widely used to investigate the origins of rice domestication and agriculture (Gu et al., 2013; Hilbert et al., 2017; Huan et al., 2015), and their characteristic production in the Oryzeae is supported in this study.

Tall tower rondels (RON-1 and RON-2) are also common in the culm of *O. meridionalis* (Supplementary Material Fig. S2). Although some studies have observed distinct rondels in other members of the Oryzeae (Ghosh et al., 2011; Gu et al., 2013; Yost and Blinnikov, 2011), no distinctive features were noted here. Many rondels in rice species have distinct characteristics that distinguish them from those of the Pooideae subfamily but show high morphological similarity to those of the Panicoideae, which is supported in this study (Piperno, 2006).

6.2.8. Arundinoideae subfamily, genus Phragmites

The subfamily Arundinoideae is represented in this study by two species of the genus *Phragmites*. Tall saddles (SAD-5) are exclusively present in these species and are particularly abundant in leaves (Fig. 3; Supplementary Material Fig. S2). Tall saddles are widely reported in this genus, equivalent to the morphotype 5-F of Cordova (2013), S-4 and S-5 of Novello et al. (2012), and the plateaued saddles of Piperno and Pearsall (1998). This morphotype has also been reported in low amounts from some Chloridoideae grasses (Novello et al., 2012; Ghosh et al., 2011; Lu and Liu, 2003), but was not reported in the Arundinoideae species *Arundo donax* by Ollendorf et al., 1988. We therefore propose that tall saddles (SAD-5) can be used as a marker of the genus *Phragmites* (see Section 6.4).

Phragmites species also produce distinct flabellate bulliform morphotypes (Plate I 59). Chen et al. (2020) suggests that the bulliforms of *Phragmites* species can be characterised by their round, large bottoms and pointed top, without distinct indentations along the edges. The distinct nature of these morphotypes from both other Arundinoideae members and other subfamilies is supported by Chen et al. (2020) and Lu et al. (2006). This morphotype can be used as a marker of *Phragmites* genus when found alongside tall saddles.

Additionally, the culm and inflorescence of *Phragmites* species show high frequencies of tall tower (RON-2) morphotypes (Fig. 3; Supplementary Material Fig. S2). These morphotypes were widely distributed across subfamilies in this study and show no significant taxonomic or environmental affiliation, although they appear to be most abundant in C_3 grasses (see Section 6.4).

6.3. Environmental significance of morphotypes

Distribution of species and morphotypes in the DCA biplot largely reflects the environmental gradient along which specimens were collected (Fig. 1; Fig. 5). Grass lineages typically have well defined biogeographic associations, primarily controlled by temperature,

precipitation, water availability, and soil texture (Groves, 1994; Lehmann et al., 2019; Edwards and Smith, 2010). These results suggest that grass phytolith assemblages may be used as proxies for the environmental conditions associated with some grass types (see Section 6.4). This study is limited to focus on C$_4$ grasses, as over 95% of grasses within the NT follow this pathway (Hattersley, 1983). Future investigations of C$_3$ grass phytolith production may help to improve the ecological resolution of GSSCP morphotypes but is beyond the scope of this study as they are uncommon in northern Australia.

Phragmites and *Oryza* species, the only C$_3$ grasses in this study, are restricted to at least seasonally wet, aquatic habitats and are particularly abundant in the wetlands of the far north NT (Groves and Whalley, 2002; ALA, 2021). This distinct environmental association is reflected in Fig. 5. However, *Phragmites* species (and the Arundinoideae subfamily generally) show no strong relationship with precipitation globally, occurring in aquatic environments regardless of total MAP (Taub, 2000; ALA, 2021). Accordingly, they are found in NT semi-arid localities with sufficient local non-climatic moisture availability, for example along the Finke River south of Alice Springs (ALA, 2021). The presence of the GSSCP markers for these species (SAD-5, BIL-9) are widely used as indicators of aquatic habitats, particularly wetlands (Yost and Blinnikov, 2011; Hilbert et al., 2017; Novello et al., 2012).

Comparatively, *Aristida* and Chloridoideae species, although widely distributed across the NT, have highest species richness and are dominant in the semi-arid zone (Fig. 1) (Groves and Whalley, 2002; Bryceson et al., 2023). Worldwide, the Chloridoideae and Aristidoideae subfamilies are associated with semi-arid to arid regions of high temperatures and low precipitation (Taub, 2000; Visser et al., 2012; Lehmann et al., 2019). Some Chloridoideae species are associated with locally wet habitats (Visser et al., 2012), and this subfamily is common in coastal or lakeshore environments across the NT (Groves and Whalley, 2002; Groves, 1994). Aristidoideae grasses are generally associated with disturbed environments and sandy soils (Groves, 1994; Visser et al., 2012). Both subfamilies are distributed across semi-arid sandplain and savanna ecosystems, which is reflected in the DCA (Fig. 5).

The Triodiinae subtribe occupies a distinct niche in Australian landscapes, with hummock grasslands covering one-third of the continent (Bradstock et al., 2012). *Triodia* grasses generally are found in semi-arid to arid regions on infertile or rocky substrates, dominating where MAP is < 250 mm per year, although some species (e.g., *T. bitextura*) are restricted to tropical regions on rocky substrates (Groves, 1994; Bowman et al., 2010; Bradstock et al., 2012; ALA, 2021). This wide distribution is reflected in the DCA biplot, with no distinct community affiliation (Fig. 5). The high variability in phytolith production patterns within this genus additionally complicates interpreting environmental conditions. The morphotype RON-8a appears to be more common in arid species (e.g., *T. basedowii),* while BIL-7 is more common in the widespread (e.g., *T. pungens)* and tropical (e.g., *T. bitextura)* species. The presence of markers of this genus may generally indicate drier conditions and/or infertile substrates, but consideration of overall assemblage composition is necessary for best environmental interpretation. Further studies of this genus are needed to better understand phytolith production patterns and resolve the taxonomic and environmental significance of associated morphotypes.

The numerous morphotypes produced by the Panicoideae subfamily may reflect their wide distribution and environmental tolerances across the NT region. The Andropogoneae tribe has highest species richness in the far north tropical savannas, where they dominate understorey grass communities (Groves and Whalley, 2002; Hutley et al., 2011; Bryceson et al., 2023). This tribe is strongly associated worldwide with high MAP (peaking at ~ 1200 mm) as well as frequent fire regimes (Lehmann et al., 2019; Taub, 2000; Visser et al., 2012). The Paniceae tribe is similar but has a secondary centre of species richness in central Australia (Bryceson et al., 2023), where many of the Paniceae specimens in this study were collected (Table 1). The dominance of this subfamily in far north tropical savannas is reflected in the DCA biplot (Fig. 5), but ecological groups

within the subfamily cannot be distinguished. A mix of Panicoideae and Chloridoideae species characterise the understorey of semi-arid savannas (Groves and Whalley, 2002; Hutley et al., 2011), as seen in Fig. 5. The presence of (abundant) Panicoideae subfamily markers (BIL-15, CRO-4 to 7) may therefore indicate higher precipitation conditions as well as savanna ecosystems.

The *Eriachne* genus is widely distributed across the NT (ALA, 2021). Many species are particularly common in savanna environments. The genus tends to occupy drier, open habitats with poor soils which characterise much of the NT (Groves and Whalley, 2002). Therefore, despite the high taxonomic significance of their exclusive morphotypes (BIL-18, RON-7), these morphotypes have low environmental significance.

6.4. Relevance for palaeoecological reconstruction

Based on the analyses performed in this study, a detailed GSSCP classification system is presented for future palaeoecological reconstruction in this region (Fig. 7). This system includes those markers of taxonomic and/or environmental significance, as well as commonly occurring and co-occurring morphotypes, while aiming to reduce the large time and effort expenditures used in identifying a range of phytolith morphotypes. Such resolution of grass taxonomy and ecology constitutes an important improvement for examining palaeoecological change in Australian grassy ecosystems.

We propose that GSSCP morphotypes BIL-15, CRO-4, CRO-5, CRO-6 and CRO-7 may be used as indicators of the Panicoideae in northern Australia, as well as for tropical savanna communities and higher precipitation conditions. Based on morphotype co-occurrence data, we also suggest RON-4, BIL-2, and BIL-3 as indicators of savanna communities when found together with Panicoideae GSSCPs. GSSCP morphotypes characteristic of the Chloridoideae (SAD-1, SAD-2) together with morphotypes diagnostic of the *Aristida* genus (Aristidoideae) (BIL-14, POL-5) appear to be useful indicators of semi-arid to arid environments in the region. RON-3 may be a useful indicator of these environmental conditions due to its prevalence and co-occurrence patterns in these two subfamilies. While multiple distinct GSSCP were identified in the Triodiinae subtribe (RON-8, BIL-7, BIL-12) and *Eriachne* genus (Micrairoideae) (RON-7, BIL-18), their environmental affiliations are unclear. Finally, we propose GSSCP morphotypes SAD-5 and BIL-9 as markers of the genus *Phragmites* (Arundinoideae) and Oryzeae tribe (Oryzoideae) respectively, alongside distinct flabellate bulliform phytoliths. Together, these morphotypes may as used as indicators of aquatic localities in northern Australia.

7. Conclusions

The application of a detailed GSSCP classification and multivariate morphospace analysis reveals distinct patterns of morphotype production among grass subfamilies, tribes, and genera in northern Australia. Some morphotypes can be used as markers of certain subfamilies (Panicoideae, Chloridoideae), and genera (*Oryza, Aristida, Phragmites, Eriachne, Triodia*). Identification of morphological variations of GSSCP categories reduces the redundancy of these morphotypes across subfamilies, while morphotype co-occurrence analysis reveals distinct patterns of GSSCP assemblage composition between grass subfamilies and tribes.

The analysis of species within a multivariate morphospace suggests that phytolith assemblages reflect environmental conditions associated with grass taxa, particularly in terms of precipitation and moisture availability. Semi-arid, sandy conditions associated with abundance of Chloridoideae and *Aristida* grasses can be statistically differentiated from the tropical, wetter conditions where Panicoideae grasses are dominant, as well as the aquatic conditions of *Oryza* and *Phragmites* species. Statistical analyses indicate a significant influence of mean annual precipitation on the dataset, reflecting the aridity gradient driving modern ecological distribution in the Northern Territory. This
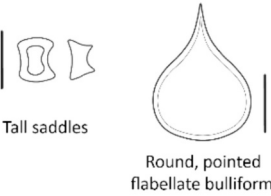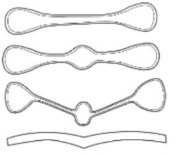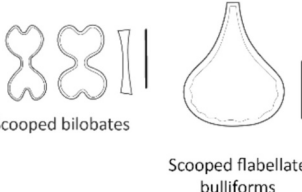
Fig. 7. Phytolith morphotype classification scheme for palaeoecological reconstruction of grassy ecosystems in northern Australia.

study supports the use of fossil phytolith analysis as a tool for palaeoecological reconstructions in this region.

Declaration of competing interest

The authors declare that they have no known competing financial interests or personal relationships that could have appeared to influence the work reported in this paper.

Data availability

Data will be made available on request.

Acknowledgements

Appendix A. Supplementary data

Supplementary data to this article can be found online at https://doi.org/10.1016/j.revpalbo.2024.105169.

References

Atlas of Living Australia (ALA), 2021. Open Access to Australia's Biodiversity Data. Available from. https://www.ala.org.au/.

Barboni, D., Bremond, L., 2009. Phytoliths of East African grasses: an assessment of their environmental and taxonomic significance based on floristic data. Rev. Palaeobot. Palynol. 158 (1), 29–41. https://doi.org/10.1016/j.revpalbo.2009.07.002.

Bird, M.I., Hutley, L.B., Lawes, M.J., Lloyd, J., Luly, J.G., Ridd, P.V., Roberts, R.G., Ulm, S., Wurster, C.M., 2013. Humans, megafauna and environmental change in tropical Australia: humans, megafauna and environmental change in tropical Australia. J. Quat. Sci. 28 (5), 439–452. https://doi.org/10.1002/jqs.2639.

Bird, M.I., Brand, M., Comley, R., Fu, X., Hadeen, X., Jacobs, Z., Rowe, C., Wurster, C.M., Zwart, C., Bradshaw, C.J., 2024. Late Pleistocene emergence of an anthropogenic fire regime in Australia's tropical savannahs. Nat. Geosci. 17 (3), 233–240.

Bourel, B., Novello, A., 2020. Bilobate phytolith size matters for taxonomical and ecological identification of Chad grasses: a case study on 15 species. Rev. Palaeobot. Palynol. 275, 104114 https://doi.org/10.1016/j.revpalbo.2019.104114.

Bowdery, D., 1998. Phytolith Analysis Applied to Pleistocene-Holocene Archaeological Sites in the Australian Arid Zone. BAR Publishing. https://doi.org/10.30861/9780860549345.

Bowman, D.M.J.S., Brown, G.K., Braby, M.F., Brown, J.R., Cook, L.G., Crisp, M.D., Ford, F., Haberle, S., Hughes, J., Isagi, Y., Joseph, L., McBride, J., Nelson, G., Ladiges, P.Y., 2010. Biogeography of the Australian monsoon tropics. J. Biogeogr. 37 (2), 201–216. https://doi.org/10.1111/j.1365-2699.2009.02210.x.

Boyd, W.E., 1990. Quaternary pollen analysis in the arid zone of Australia: Dalhousie Springs, Central Australia. Rev. Palaeobot. Palynol. 64 (1–4), 331–341. https://doi.org/10.1016/0034-6667(90)90149-D.

Bradstock, R.A., Williams, R.J., Gill, A.M., 2012. Future fire regimes of Australian ecosystems: new perspectives on enduring questions of management. *Flammable Australia: fire regimes, biodiversity and ecosystems in a changing world*, pp. 307–324.

Bryceson, S.R., Hemming, K.T.M., Duncan, R.P., Morgan, J.W., 2023. The contemporary distribution of grasses in Australia: a process of immigration, dispersal and shifting dominance. J. Biogeogr. 50 (9), 1639–1652. https://doi.org/10.1111/jbi.14676.

Bureau of Meteoroloy, 2023. Climate Data Online. http://www.bom.gov.au/climate/data/.

Chen, I., Li, K., Tsang, C., 2020. Silicified bulliform cells of Poaceae: morphological characteristics that distinguish subfamilies. Bot. Stud. 61 (1), 5. https://doi.org/10.1186/s40529-020-0282-x.

Cheney, P., Sullivan, A., 2008. Grassfires: Fuel, Weather and Fire Behaviour. Csiro Publishing.

Cordova, C.E., 2013. C3 Poaceae and Restionaceae phytoliths as potential proxies for reconstructing winter rainfall in South Africa. Quat. Int. 287, 121–140. https://doi.org/10.1016/j.quaint.2012.04.022.

Cordova, C.E., Scott, L., 2010. The potential of Poaceae, Cyperaceae and Restionaceae phytoliths to reflect past environmental conditions in South Africa. In: African Palaeoenvironments and Geomorphic Landscape Evolution. CRC Press, pp. 133–160.

Crabtree, S.A., White, D.A., Bradshaw, C.J., Saltr`e, F., Williams, A.N., Beaman, R.J., Bird, M.I., Ulm, S., 2021. Landscape rules predict optimal superhighways for the first peopling of Sahul. Nat. Hum. Behav. 5, 1303–1313. https://doi.org/10.1038/s41562-021-01106-8.

Edwards, E.J., Smith, S.A., 2010. Phylogenetic analyses reveal the shady history of C4 grasses. Proc. Natl. Acad. Sci. 107 (6), 2532–2537. https://doi.org/10.1073/pnas.0909672107.

Ehleringer, J.R., 2005. In: *A history of atmospheric CO$_2$ and its effects on plants, animals, and ecosystems*. The influence of atmospheric CO$_2$, temperature, and water on the abundance of C3/C4 taxa. Springer New York, New York, NY, pp. 214–231.

Fahmy, A.G., 2008. Diversity of lobate phytoliths in grass leaves from the Sahel region, West Tropical Africa: Tribe Paniceae. Plant Syst. Evol. 270 (1), 1–23. https://doi.org/10.1007/s00606-007-0597-z.

Fujiwara, H., Jones, R., Brockwell, C.J., 1985. Plant Opals (Phytoliths) in Kakadu Archaeological Sites: A Preliminary Report.

Ghosh, R., Naskar, M., Bera, S., 2011. Phytolith assemblages of grasses from the Sunderbans, India and their implications for the reconstruction of deltaic environments. Palaeogeogr. Palaeoclimatol. Palaeoecol. 311 (1), 93–102. https://doi.org/10.1016/j.palaeo.2011.08.009.

Griffith, D.M., Veech, J.A., Marsh, C.J., 2016. Cooccur: probabilistic species co-occurrence analysis in R. J. Stat. Softw. 69 (2), 1–17. https://doi.org/10.18637/jss.v069.c02.

Groff, D.V., Greenawalt, K.E., Gill, J.L., 2022. Grass pollen and phytoliths of the Falkland Islands. Rev. Palaeobot. Palynol. 299, 104603 https://doi.org/10.1016/j.revpalbo.2022.104603.

Groves, R.H. (Ed.), 1994. Australian Vegetation. Cambridge University Press.

Groves, R.H., Whalley, R.D.B., 2002. Grass and grassland ecology in Australia. Flora of Australia 43, 157–182.

Gu, Y., Zhao, Z., Pearsall, D.M., 2013. Phytolith morphology research on wild and domesticated rice species in East Asia. Quat. Int. 287, 141–148. https://doi.org/10.1016/j.quaint.2012.02.013.

Hart, D.M., 1990. Occurence of the 'Cyperaceae-type' phytolith in dicotyledons. Aust. Syst. Bot. 3 (4), 745–750.

Hart, D.M., 1997. Phytoliths and Fire in the Sydney Basin, New South Wales (Australia), pp. 101–110.

Hattersley, P.W., 1983. The distribution of C3 and C4 grasses in Australia in relation to climate. Oecologia 57 (1–2), 113–128. https://doi.org/10.1007/BF00379569.

Hilbert, L., Neves, E.G., Pugliese, F., Whitney, B.S., Shock, M., Veasey, E., Zimpel, C.A., Iriarte, J., 2017. Evidence for mid-Holocene rice domestication in the Americas. Nat. Ecol. Evol. 1 (11) https://doi.org/10.1038/s41559-017-0322-4. Article 11.

Huan, X., Lu, H., Wang, C., Tang, X., Zuo, X., Ge, Y., He, K., 2015. Bulliform phytolith research in wild and domesticated rice paddy soil in South China. PloS One 10 (10), e0141255. https://doi.org/10.1371/journal.pone.0141255.

Hutley, L.B., Beringer, J., Isaac, P.R., Hacker, J.M., Cernusak, L.A., 2011. A sub-continental scale living laboratory: spatial patterns of savanna vegetation over a rainfall gradient in northern Australia. Agric. For. Meteorol. 151 (11), 1417–1428. https://doi.org/10.1016/j.agrformet.2011.03.002.

International Committee for Phytolith Taxonomy (ICPT), 2019. International Code for Phytolith Nomenclature (ICPN) 2.0. Ann. Bot. 124 (2), 189–199. https://doi.org/10.1093/aob/mcz064.

Lehmann, C.E.R., Griffith, D.M., Simpson, K.J., Anderson, T.M., Archibald, S., Beerling, D.J., Bond, W.J., Denton, E., Edwards, E.J., Forrestel, E.J., Fox, D.L., Georges, D., Hoffmann, W.A., Kluyver, T., Mucina, L., Pau, S., Ratnam, J., Salamin, N., Santini, B., Osborne, C.P., 2019. Functional diversification enabled grassy biomes to fill global climate space, p. 583625. In: bioRxiv. https://doi.org/10.1101/583625.

Llewelyn, J., Strona, G., McDowell, M.C., Johnson, C.N., Peters, K.J., Stouffer, D.B., de Visser, S.N., Saltr`e, F., Bradshaw, C.J., 2021. Sahul's megafauna were vulnerable to plant-community changes due to their position in the trophic network. Ecography 2022, 1–15. https://doi.org/10.1111/ecog.06089.

Lu, H., Liu, K.-B., 2003. Morphological variations of lobate phytoliths from grasses in China and the south-eastern United States. Divers. Distrib. 9 (1), 73–87.

Lu, H.Y., Wu, N.Q., Yang, X.D., Jiang, H., Liu, K.B., Liu, T.S., 2006. Phytoliths as quantitative indicators for the reconstruction of past environmental conditions in China I: phytolith-based transfer functions. Quaternary Science Reviews 25 (9–10), 945–959.

Ma, X., Huete, A., Yu, Q., Coupe, N.R., Davies, K., Broich, M., Ratana, P., Beringer, J., Hutley, L.B., Cleverly, J., Boulain, N., Eamus, D., 2013. Spatial patterns and temporal dynamics in savanna vegetation phenology across the North Australian Tropical Transect. Remote Sens. Environ. 139, 97–115. https://doi.org/10.1016/j.rse.2013.07.030.

MacPhail, M.K., Hill, R.S., 2002. Palaeobotany of the Poaceae. In: Flora of Australia, 43, pp. 37–70.

Madella, M., Alexandre, A., Ball, T., ICPN Working Group, 2005. International Code for Phytolith Nomenclature 1.0. Ann. Bot. 96 (2), 253–260. https://doi.org/10.1093/aob/mci172.

Mariani, M., Connor, S.E., Theuerkauf, M., Herbert, A., Kuneš, P., Bowman, D., Fletcher, M., Head, L., Kershaw, A.P., Haberle, S.G., Stevenson, J., Adeleye, M., Cadd, H., Hopf, F., Briles, C., 2022. Disruption of cultural burning promotes shrub encroachment and unprecedented wildfires. Front. Ecol. Environ. fee.2395 https://doi.org/10.1002/fee.2395.

Munroe, S.E.M., Guerin, G.R., McInerney, F.A., Martín-Forés, I., Welti, N., Farrell, M., Atkins, R., Sparrow, B., 2022. A vegetation carbon isoscape for Australia built by combining continental-scale field surveys with remote sensing. Landsc. Ecol. 37 (8), 1987–2006. https://doi.org/10.1007/s10980-022-01476-y.

Murungi, M.L., Bamford, M.K., 2020. Revised taxonomic interpretations of Cyperaceae phytoliths for (paleo)botanical studies with some notes on terminology. Rev. Palaeobot. Palynol. 275, 104189 https://doi.org/10.1016/j.revpalbo.2020.104189.

Neumann, K., Fahmy, A.G., Müller-Scheeßel, N., Schmidt, M., 2017. Taxonomic, ecological and palaeoecological significance of leaf phytoliths in West African grasses. Quat. Int. 434, 15–32. https://doi.org/10.1016/j.quaint.2015.11.039.

Novello, A., Barboni, D., 2015. Grass inflorescence phytoliths of useful species and wild cereals from sub-Saharan Africa. J. Archaeol. Sci. 59, 10–22. https://doi.org/10.1016/j.jas.2015.03.031.

Novello, A., Barboni, D., Berti-Equille, L., Mazur, J.-C., Poilecot, P., Vignaud, P., 2012. Phytolith signal of aquatic plants and soils in Chad, Central Africa. Rev. Palaeobot. Palynol. 178, 43–58. https://doi.org/10.1016/j.revpalbo.2012.03.010.

Oksanen, J., Simpson, G., Blanchet, F., Kindt, R., Legendre, P., Minchin, P., O'Hara, R., Solymos, P., Stevens, M., Szoecs, E., Wagner, H., Barbour, M., Bedward, M., Bolker, B., Borcard, D., Carvalho, G., Chirico, M., De Caceres, M., Durand, S., Evangelista, H., FitzJohn, R., Friendly, M., Furneaux, B., Hannigan, G., Hill, M., Lahti, L., McGlinn, D., Ouellette, M., Ribeiro Cunha, E., Smith, T., Stier, A., Ter Braak, C., Weedon, J., 2022. Vegan: Community Ecology Package. R Package Version 2.6-4. https://CRAN.R-project.org/package=vegan.

Ollendorf, A.L., 1992. Toward a classification scheme of sedge (Cyperaceae) phytoliths. In: Rapp, G., Mulholland, S.C. (Eds.), Phytolith Systematics: Emerging Issues. Springer US, pp. 91–111. https://doi.org/10.1007/978-1-4899-1155-1_5.

Parr, J., Watson, L., 2007. Morphological characteristics observed in the leaf phytoliths of selected Gymnosperms of eastern Australia. In: Plants, People and Places-Recent Studies in Phytoliths Analysis. Oxbow Books, p. 272.

Ollendorf, A.L., Mulholland, S.C., Rapp Jr., G., 1988. Phytolith analysis as a means of plant identification: Arundo donax and Phragmites communis. Annals of Botany 61 (2), 209–214.

Parr, J.F., Lentfer, C.J., Boyd, W.E., 2001. A comparative analysis of wet and dry ashing techniques for the extraction of phytoliths from plant material. J. Archaeol. Sci. 28 (8), 875–886. https://doi.org/10.1006/jasc.2000.0623.

Pearsall, D.M., Piperno, D.R., Dinan, E.H., Umlauf, M., Zhao, Z., Benfer, R.A., 1995. Distinguishing rice (*Oryza sativa* Poaceae) from wild Oryza species through phytolith analysis: results of preliminary research. Econ. Bot. 49 (2), 183–196.

Piperno, D.R., 1989. The occurrence of phytoliths in the reproductive structures of selected tropical angiosperms and their significance in tropical paleoecology, paleoethnobotany and systematics. Review of Palaeobotany and Palynology 61 (1–2), 147–173.

Piperno, D.R., 2006. Phytoliths: A Comprehensive Guide for Archaeologists and Paleoecologists. Rowman Altamira.

Piperno, D.R., Pearsall, D.M., 1998. The silica bodies of tropical American grasses: morphology, taxonomy, and implications for grass systematics and fossil phytolith identification. Smithson. Contrib. Bot. 1, 1–40.

Reeves, J.M., Barrows, T.T., Cohen, T.J., Kiem, A.S., Bostock, H.C., Fitzsimmons, K.E., Jansen, J.D., Kemp, J., Krause, C., Petherick, L., 2013. Climate variability over the last 35,000 years recorded in marine and terrestrial archives in the Australian region: an OZ-INTIMATE compilation. Quat. Sci. Rev. 74, 21–34.

RStudio Team, 2022. RStudio: Integrated Development Environment for R. RStudio, PBC, Boston, MA. URL. http://www.rstudio.com/.

Salles, T., Joannes-Boyau, R., Moffat, I., Husson, L., Lorcery, M., 2024. Physiography, foraging mobility, and the first peopling of Sahul. Nat. Commun. 15, 3430. https://doi.org/10.1038/s41467-024-47662-1.

Schlesinger, C., White, S., Muldoon, S., 2013. Spatial pattern and severity of fire in areas with and without buffel grass (Cenchrus ciliaris) and effects on native vegetation in central Australia. Austral Ecol. 38 (7), 831–840. https://doi.org/10.1111/aec.12039.

Setterfield, S.A., Rossiter-Rachor, N.A., Douglas, M.M., Wainger, L., Petty, A.M., et al., 2013. Adding fuel to the fire: the impacts of non-native grass invasion on fire management at a regional scale. PloS One 8 (5), e59144. https://doi.org/10.1371/journal.pone.0059144.

Singh, G., 1981. Late Quaternary pollen records and seasonal palaeoclimates of Lake Frome, South Australia. In: Williams, W.D. (Ed.), Salt Lakes, pp. 419–430. Springer Netherlands. https://doi.org/10.1007/978-94-009-8665-7_29.

Soreng, R.J., Peterson, P.M., Romaschenko, K., Davidse, G., Teisher, J.K., Clark, L.G., Barberá, P., Gillespie, L.J., Zuloaga, F.O., 2017. A worldwide phylogenetic classification of the Poaceae (Gramineae) II: an update and a comparison of two 2015 classifications. J. Syst. Evol. 55 (4), 259–290. https://doi.org/10.1111/jse.12262.

Stevanato, M., Rasbold, G.G., Parolin, M., Domingos Luz, L., Lo, E., Weber, P., Trevisan, R., Galeazzi Caxambu, M., 2019. New characteristics of the papillae phytolith morphotype recovered from eleven genera of cyperaceae. Flora 253, 49–55. https://doi.org/10.1016/j.flora.2019.03.012.

Strömberg, C.A.E., Dunn, R.E., Crifò, C., Harris, E.B., 2018. Phytoliths in paleoecology: analytical considerations, current use, and future directions. In: Croft, D.A., Su, D.F., Simpson, S.W. (Eds.), Methods in Paleoecology: Reconstructing Cenozoic Terrestrial Environments and Ecological Communities. Springer International Publishing, pp. 235–287. https://doi.org/10.1007/978-3-319-94265-0_12.

Taub, D.R., 2000. Climate and the U.S. distribution of C4 grass subfamilies and decarboxylation variants of C4 photosynthesis. Am. J. Bot. 87 (8), 1211–1215. https://doi.org/10.2307/2656659.

Turnbull, M., Parker, A.G., Jankowski, N.R., 2023. The history of phytolith research in Australasian archaeology and palaeoecology. Veg. Hist. Archaeobotany. https://doi.org/10.1007/s00334-023-00922-4.

Visser, V., Woodward, F.I., Freckleton, R.P., Osborne, C.P., 2012. Environmental factors determining the phylogenetic structure of C4 grass communities. J. Biogeogr. 39 (2), 232–246. https://doi.org/10.1111/j.1365-2699.2011.02602.x.

Wallis, L.A., 2000. Phytoliths, Late Quaternary Environment and Archaeology in Tropical Semi-Arid Northwest Australia. https://doi.org/10.25911/5d5fccf93672d.

Wallis, L., 2003. An overview of leaf phytolith production patterns in selected northwest Australian flora. Rev. Palaeobot. Palynol. 125 (3), 201–248. https://doi.org/10.1016/S0034-6667(03)00003-4.

Williams, Duff, G.A., Bowman, D.M.J.S., Cook, G.D., 1996. Variation in the composition and structure of tropical savannas as a function of rainfall and soil texture along a large-scale climatic gradient in the Northern Territory, Australia. J. Biogeogr. 23 (6), 747–756. https://doi.org/10.1111/j.1365-2699.1996.tb00036.x.

Yost, C.L., Blinnikov, M.S., 2011. Locally diagnostic phytoliths of wild rice (*Zizania palustris* L.) from Minnesota, USA: comparison to other wetland grasses and usefulness for archaeobotany and paleoecological reconstructions. J. Archaeol. Sci. 38 (8), 1977–1991. https://doi.org/10.1016/j.jas.2011.04.016.